31st Annual International Conference of the IEEE EMBS
Minneapolis, Minnesota, USA, September 2-6, 2009

Real-time Identification and Visualization of Human Segment Parameters

Gentiane Venture [1], Ko Ayusawa[2], Yoshihiko Nakamura[2]

***Abstract*— Mass parameters of the body segments are mandatory to study motion dynamics. No systematic method to estimate them has been proposed so far. Rather, parameters are scaled from generic tables or estimated with methods inappropriate for in-patient care. Based on our previous works, we propose a real-time software that allows to estimate the whole-body segment parameters, and to visualize the progresses of the completion of the identification. The visualization is used as a feedback to optimize the excitation and thus the identification results. The method is experimentally tested.**

I. Introduction

When studying human motions dynamics the appropriate knowledge of segment parameters (SP) is mandatory. Such is the case in orthopedics, biomechanics, neurology. With an accurate knowledge of the subject specific segment parameter is is possible to refine diagnosis and personalize health-care. The trajectory of the whole-body center of mass (COM) is also often use in gait studies; the computation of the SP: inertia and the position of the COM of each link of the body, is a key-step in gait analysis and to monitor the SP variations due to disease, hospitalization, rehabilitation or training [1]. Systems to estimate in-vivo the position of the whole-body COM have been recently released [2], [3]. Nevertheless, the inertias are usually not estimated in-vivo, by lack of accurate methodology, and are computed by interpolations of data [4]. These data is obtained by photogrammetry [5] or by 3D imaging (CT-scan or MRI) and 3D modeling interpolations [6]. Discrepancies in body landmarks and in models [7] as well as the profusion of references make an adequate choice difficult. In addition, proper interpolations of the available data require massive geometric measurements. Finally, it is shown in [8] that errors in the body-segment mass-parameter affect significantly the analysis results. Consequently, there is a urge to estimate in-vivo and accurately the SP of the human body. Based on our previous works [9], we present here a methodology for real-time (RT) estimation of the SP from motion and contact force [10]. A graphic interface is used to generate persistent exciting trajectories from visual feedback. This method allows in-vivo subject-specific identification of the SP with a fast, safe and robust environment. It makes use of both the identification of the base-parameters and an interpolation from data extracted from the data-base of human body.

This research was supported by the Special Coordination Funds for Promoting Science and Technology: "IRT Foundation to Support Man and Aging Society".

[1] Department of Mechanical System Engineering, Tokyo University of Agriculture and Technology
[2] Department of Mechano-Informatics, The University of Tokyo, Japan
venture@cc.tuat.ac.jp

II. Identification from contact forces and motion data

A. Identification model of legged systems

The original identification method of the base parameters has been described in our previous work [9]. We use this method to obtain the minimal identification for the human body given respectively by Eq. 1 and Eq. 2.

$$\boldsymbol{Y}_O\boldsymbol{\phi} = \sum_{k=1}^{N_c} \boldsymbol{J}_{Ok}^T \boldsymbol{F}_k^{ext} \qquad (1)$$

$$\boldsymbol{\phi}_B = \boldsymbol{Z}\boldsymbol{\phi} \qquad (2)$$

where:

- N_c is the number of contact with the environment,
- $\boldsymbol{F}_k^{ext} \in \boldsymbol{R}^6$ is the vector of external forces exerted to the humanoid at contact k,
- $\boldsymbol{J}_{Ok} \in \boldsymbol{R}^{6\times6}$ is the basic Jacobian matrices of the position at contact k and of the orientation of the contact link with respect to $\boldsymbol{q_0}$ and $\boldsymbol{q_c}$, which are used to map $\boldsymbol{F}_k^{ext}$ to the vector of generalized forces.
- $\boldsymbol{\phi} \in \boldsymbol{R}^{10n}$ is the vector of segment parameters (SP).
- $\boldsymbol{Y}_O \in \boldsymbol{R}^{6\times10n}$ is the regressor for the base-link, a function matrix of generalized coordinates $\boldsymbol{q_0}$ of the base-link, the joint angles $\boldsymbol{q_c}$, and their derivatives $\dot{\boldsymbol{q}}_0$, $\dot{\boldsymbol{q}}_c$, $\ddot{q}_0$, $\ddot{q}_c$. $\boldsymbol{Y}_O \in \boldsymbol{R}^{6\times10n}$ is the regressor corresponding in the six equations of motion of the base-link.
- $\boldsymbol{Z} \in \boldsymbol{R}^{N_B\times10n}$ is the composition matrix of base parameters [11]. $\boldsymbol{Y}_B \in \boldsymbol{R}^{N_J\times N_B}$ is called the regressor for the base parameters and is of full-rank.

B. Estimation of whole-body SP

Identification using Eq. 1 gives only the base parameters $\boldsymbol{\phi}_B$. They $\boldsymbol{\phi}_B$ are the necessary and sufficient information to compute the equations of motion. However, they are often too complicated to be comprehended straightforwardly with physiological meaning. The standard SP $\boldsymbol{\phi}$ are more comprehensible $\boldsymbol{\phi}_B$ as they are the straightforward expression of the mass and moment of inertia. We propose to estimate the SP after the identification of the base parameters $\hat{\boldsymbol{\phi}}_B$, by extrapolating literature data or data-base. The estimated standard parameters meet the base-parameters without distortion. For the linear equation (2), the general form of the least-squares solution for a rank-deficient regressor is given by [12]:

$$\boldsymbol{\phi} = \boldsymbol{Z}^{\#}\phi_B + (\boldsymbol{E} - \boldsymbol{Z}^{\#}\boldsymbol{Z})\boldsymbol{z} \qquad (3)$$

where $\boldsymbol{z} \in \boldsymbol{R}^{10n}$ is an arbitrary vector, and $\boldsymbol{E}$ is the identity matrix. When using the identified base parameters $\hat{\phi}_B$, the main problem resides in determining the vector $\boldsymbol{z}$ projected to the null space of the composition matrix $\boldsymbol{Z}$. We choose the vector $\boldsymbol{z} = \phi^{ref}$, where ϕ^{ref} is the information found in the data-base for the standard parameters or reference standard parameters, and finally the subject-specific standard parameters $\hat{\phi}$ can be obtained:

$$\begin{aligned} \hat{\phi} &= \boldsymbol{Z}^{\#}\hat{\phi}_B + (\boldsymbol{E} - \boldsymbol{Z}^{\#}\boldsymbol{Z})\phi^{ref} \\ &= \phi^{ref} + \boldsymbol{Z}^{\#}(\hat{\phi}_B - {\phi_B}^{ref}) \end{aligned} \quad (4)$$

Where, ${\phi_B}^{ref} = \boldsymbol{Z}\phi^{ref}$. Eq. 4 satisfies Eq. 2. Eq. 4 also implies that $\hat{\phi}$ minimizes $||\phi - \phi^{ref}||$, which means the error of the reference standard parameters ϕ^{ref}.

III. RT VISUALIZATION OF THE RESULTS

A. Outline

Each step is of the identification routine is detailed in the following subsections. Motions are recorded every 5[ms] by a commercial optical motion capture: 10 cameras (Motion Analysis), 35 reflective markers, and the contact forces are measured every 1[ms] by two force-plates (Kistler). The human body is modeled by a rigid body model with 34 degrees of freedom [9]. The motion-data and the force-data are synchronized. The identification process is as follows (Fig. 1):(1) the geometric model of human is defined, measure the geometric parameters of the model from motion capture, and estimate the prior standard inertial parameters from geometric parameters and data-base of human body. (2) From the motion capture and force-plates, we identify the base parameters and the standard parameters using the RT method. (3) Using colored presentation to specify the links yet not to be identified, we can improve the quality of identification results.

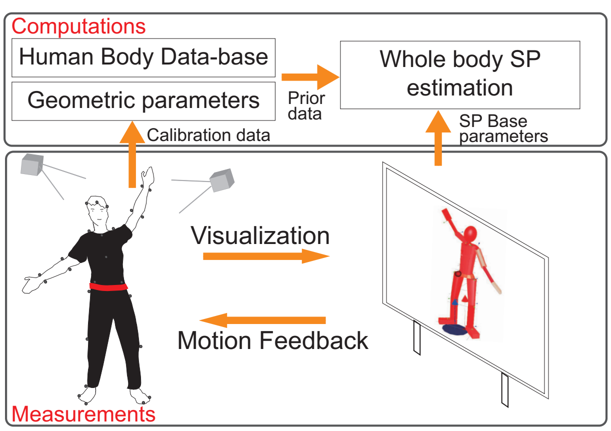

Fig. 1. Conceptual diagram of the proposed approach of RT identification and visualization

B. Estimation of the geometric model and prior estimation of standard inertial parameters

Geometric parameters are by nature measurable directly. Usually they are measured manually, here we propose to use an automatic method making use of the defined positions of the optical markers. They are located at the defined anatomical points to insure the accuracy when computing the inverse kinematics, thus we can automatically compute the geometric parameters of each link by calculating their relative position. The standard inertial parameters (reference) are then estimated from the obtained geometric model, in order to build the model shape. In this paper, we apply the method described in [13] based on the use of the data-base of the human body available from [14], to estimate the standard inertial parameters. The data-base consists in the 49 diagnostic measurements and the total body mass of 308 Japanese. The prior estimation of the standard parameters is performed as follows: (1) We measure some of the 49 diagnostic measurement and the total mass (from marker positions and force-plates data) to use as the input of the estimation routine, and then we compute the other items using a linear regression. (2) The geometric shape of the human body is modeled. In this model, each link of the human body is approximated by simple primitive shapes. For example, oval sphere, truncated cone, and boxes. (3) The size and volume of each primitive is computed from the 49 measurement items, and the inertial parameters are obtained, assuming that the density of each link is uniform.

C. On-line identification of the base parameters

From the inverse kinematics computations of marker positions, the generalized coordinates and their derivatives are obtained, the regressor is calculated RT. The total external force exerted to the frame of the base-link is calculated from the force-plates data. On-line least squares algorithm is implemented. The forces and moments in Eq. 1 have different units, and different measurement accuracies. To avoid discrepancies the weighted least squares method is used. In addition, some parameters may be time-varying, for example when a human handles or releases an object during the measurements, to identify appropriately the parameters an exponential forgetting coefficient λ_n is used. The above features are implemented as follow: At times $t = [1 \cdots n]$, the estimated parameters $\phi_{B,n}$ at $t = n$ is computed from $\phi_{B,n-1}$ at $t = n - 1$ as follow.

$$\hat{\phi}_{B,n} = \lambda_n \hat{\phi}_{B,n-1} + \boldsymbol{K}_n(\boldsymbol{F}_n - \boldsymbol{Y}_{OB,n}\hat{\phi}_{B,n-1}) \quad (5)$$

Where,

- $\lambda_n (0 \leq \lambda_n \leq 1)$ is the time-varying forgetting factor.
- $\boldsymbol{Y}_{OB,n}$ and $\boldsymbol{F}_n$ are the regressor and the external force at the time $t = n$.
- $\boldsymbol{K}_n \in \boldsymbol{R}^{N_B \times N_B}$ is the gain matrix as follow:

$$\boldsymbol{K}_n = \boldsymbol{P}_{n-1}{\boldsymbol{Y}_{OB,n}}^T{\boldsymbol{V}_n}^{-1} \quad (6)$$

- $\boldsymbol{V}_n \in \boldsymbol{R}^{6\times 6}$ is defined as follow:

$$\boldsymbol{V}_n = \lambda_n \boldsymbol{\Sigma_n} + \boldsymbol{Y}_{w,t}\boldsymbol{P}_{n-1}{\boldsymbol{Y}_{w,t}}^T \quad (7)$$

- $\boldsymbol{P}_n \in \boldsymbol{R}^{N_B \times N_B}$ is defined by defined by:

$$\boldsymbol{P}_n = \sum_{n=i}^{n}({\boldsymbol{Y}_{OB,i}}^T \boldsymbol{\Sigma}_i \boldsymbol{Y}_{OB,i})^{-1} \quad (8)$$

And the on-line inverse matrix calculation is given by:

$$\boldsymbol{P}_n = \frac{1}{\lambda_n}(\boldsymbol{P}_{n-1} - \boldsymbol{P}_{n-1}\boldsymbol{Y}_{OB,n}{}^T\boldsymbol{V}_n{}^{-1}\boldsymbol{Y}_{OB,n}\boldsymbol{P}_{n-1}) \tag{9}$$

- $\boldsymbol{\Sigma_n} \in \boldsymbol{R}^{6\times 6}$ is the weighted matrix.

The weighted matrix $\boldsymbol{\Sigma}_n$ is chosen as the covariance matrix for the disturbance of $\boldsymbol{F}$. We consider that the 6 axis elements of $\boldsymbol{F}$ are independent and thus $\boldsymbol{\Sigma}_n$ is diagonal. The i-th diagonal element $\sigma^2_{ii,n}(1 \le i \le 6)$ is the variance of the estimated error of each component of $\boldsymbol{F}$. $\sigma_{ii,n}$ can be calculated using $\boldsymbol{A}_{i,n} \in \boldsymbol{R}^{N_B\times N_B}$, $\boldsymbol{b}_{i,n} \in \boldsymbol{R}^{N_B}$, $c_{i,n} \in \boldsymbol{R}$, $d_n \in \boldsymbol{R}$ as follow, where $f_{i,n} \in \boldsymbol{R}$, $\boldsymbol{y}_{i,n} \in \boldsymbol{R}^{1\times N_B}(1 \le i \le 6)$ are the each component of respectively $\boldsymbol{F}_n$ and $\boldsymbol{Y}_{OB,n}$.

$$\sigma_{i,n}{}^2 = \frac{1}{d_n}(\boldsymbol{\phi}_{B,n-1}{}^T\boldsymbol{A}_{i,n}\boldsymbol{\phi}_{B,n-1} - 2\boldsymbol{\phi}_{B,n}{}^T\boldsymbol{b}_{i,n} + c_{i,n}) \tag{10}$$

$$\boldsymbol{A}_{i,n} = \boldsymbol{y}_{i,n}{}^T\boldsymbol{y}_{i,n} + \lambda_n^2\boldsymbol{A}_{i,n-1} \tag{11}$$

$$\boldsymbol{b}_{i,n} = f_{i,n}\boldsymbol{y}_{i,n}{}^T + \lambda_n^2\boldsymbol{b}_{i,n-1} \tag{12}$$

$$c_{i,n} = f_{i,n}{}^2 + \lambda_n^2 c_{i,n-1} \tag{13}$$

$$d_n = 1 + \lambda_n d_{n-1} \tag{14}$$

From Eq. 5, Eq. 9, and Eq. 10 - (14), we can compute $\boldsymbol{W}_n$, $\boldsymbol{P}_n$, and $\hat{\boldsymbol{\phi}}_{B,n}$ every time, and also obtain $\hat{\boldsymbol{\phi}}_n$ from Eq. 4. The initial value for $\boldsymbol{P}_0$, $\hat{\boldsymbol{\phi}}_{B0}$ and $\hat{\boldsymbol{\phi}}_0$ can be chosen as a-priori knowledge. If they are unknown, we choose $\hat{\boldsymbol{\phi}}_{B0} = \boldsymbol{0}$, $\hat{\boldsymbol{\phi}}_0 = \boldsymbol{0}$ and $\boldsymbol{P}_0 = \gamma\boldsymbol{E}$. Similarly, $\boldsymbol{A}_{i,0}, \boldsymbol{b}_{i,0}, c_{i,0}, d_{i,0}$ are chosen as zeros without a-priori data. A large value of $\gamma(> 0)$ leads to a fast convergence, nevertheless $\boldsymbol{P}_n$ becomes unstable with lack of exciting motion data. The forgetting factor λ_n is often chosen with a constant value from 0.995 to 1. If the parameters are constant (no object carried) $\lambda = 1$ is chosen (no forgetting); if the parameters are to change (when handling and releasing objects) we chose $\lambda < 1$.

D. Visualization of Persistent Excitation Trajectory

It is important to sample the identification model along a motion that excites the system dynamics to be estimated to obtain accurate SP estimates. Such motions are called Persistent Exciting Trajectories [15]. However, a large number of DOF and time-varying contact situation complicate the definition of persistent exciting trajectories [16]. The RT interface is used for the identification as well as adjustment of the persistent exciting movements. During the measurement, we display the model using a colored representation for the identified link parameters and the not yet identified link parameters. Intuitively links need to be excited are recognized. The examinee can generate the adequate persistent exciting trajectories. The colors are chosen according to the relative standard deviation calculated for each base parameter. [15], [17] The covariance matrix $\boldsymbol{C}_n \in \boldsymbol{R}^{N_B\times N_B}$ of the estimation error of $\hat{\boldsymbol{\phi}}_{B,n}$ are computed as follow:

$$\boldsymbol{C}_n = E((\boldsymbol{\phi}_B - \hat{\boldsymbol{\phi}}_{B,n})(\boldsymbol{\phi}_B - \hat{\boldsymbol{\phi}}_{B,n})^T) = \boldsymbol{P}_n \tag{15}$$

where E is the expectation operator. Eq. 5, Eq. 6, and Eq. 9 of the on-line least squares algorithm are similar to equations of a Kalman filter without the system noise, and $\boldsymbol{P}_n$ is equivalent to the covariance matrix of $\boldsymbol{C}_n$. $c_{n,(i,i)}$ is the diagonal elements of $\boldsymbol{C}_n$, and the relative standard deviation $\sigma_{\phi_j\%}$ is thus computed as follow:

$$\sigma_{\phi_j,n\%} = 100\frac{\sqrt{c_{n,(i,i)}}}{\hat{\phi}_{Bj,n}} \tag{16}$$

A parameter with a relative standard deviation $\sigma_{\phi_j\%}$ lower than a specified threshold is well identified. However for parameters with small values, they may be well identified although $\sigma_{\phi_j\%}$ is large. The results are visualized using a 3D representation of the human as defined in section III-B. Each link color changes according to a simple rule: n_{Bj} is the number of the base parameters of the link j, $n_{Bj,G}$ is the number of parameters that $\sigma_{\phi_j\%}$ is lower than 10[%], $n_{Bj,B}$ is the number of parameters that $\sigma_{\phi_j\%}$ is not lower than 10[%] but small parameters(< 0.02), and $n_{Bj,R} = n_{Bj} - n_{Bj,G} - n_{Bj,B}$. Then rgb values of each link are chosen as a ratio of $n_{Bj,R}$, $n_{Bj,G}$, and $n_{Bj,B}$. Starting from red for non identified parameters to green for fully identified parameters; and cyan for small parameters Fig. 2.

IV. Experiments

We record three motions using the RT visualization interface. During this phase the motions are free and only adjusted to provided the identification of the parameters based on the color changes. The initial conditions for RT identification are $\lambda_n = 1.0$, $\gamma = 0.001$, and other parameters are zeros.

A. Identification of base parameters

Randomly chosen motions of the whole body lead to regressor of high condition number about 500. Using the combination of several motions from a gymnastic TV program has lead to condition number about 40 [16]. Using the interface leads to obtain condition numbers of about 30. And thus to enhance the excitation properties of the recorded motions by visual feedback and the quality of the estimation. More particularly for the extremities and the head.

B. Identification of standard parameters

Table I gives some results of the estimation of the standard parameters, and initial value of literature data for the mass M[kg], the center of mass C_i[kg-m], and the inertias J_{ij}[kg-m^2] of 6 links. (L1:lower trunk, L2:upper trunk, L3:right foot, L4:right hand, L5:head, L6: right upper leg) The estimated masses are in the range of the prior parameters, and the inertias of $L2$, $L3$, $L4$ also show good correlations and are meaningful. However, the center of mass of $L1$ and $L5$, and the inertia around the Z-axis of $L1$,$L5$ and $L6$ have failed to be estimated, i.e. the center of mass is located outside of the link and the principal moment of inertia around Z-axis is negative. This can be explained as follow: some base parameters of $L1$ and $L6$ have a standard deviation higher than 15%. In addition, the prior standard parameters are not accurate and the data-base is not complete, which affects the estimated standard parameters. Though the base parameters are well identified the standard parameters reconstruction from the data base needs to be improved, more particularly

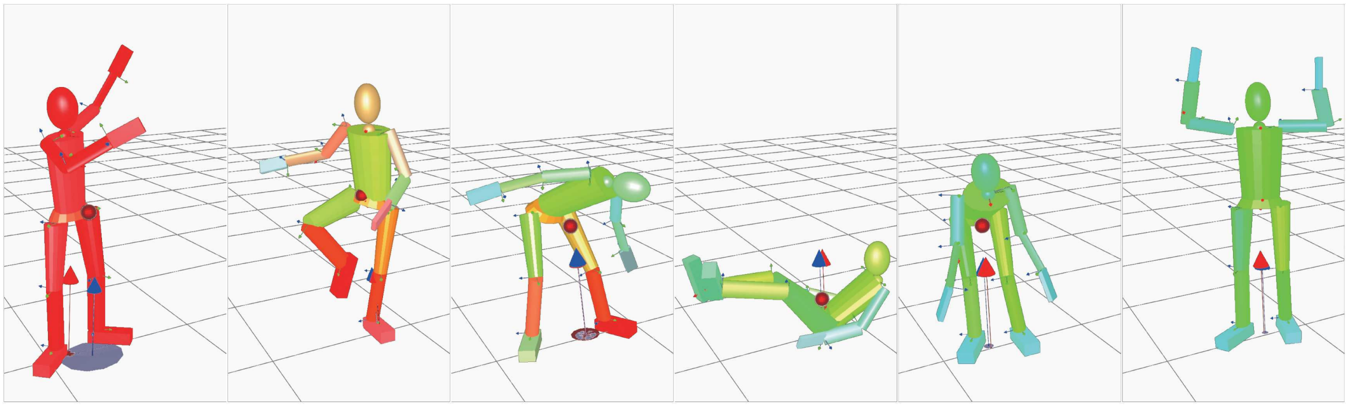

Fig. 2. RT identification of human inertial parameters

TABLE I

ESTIMATED STANDARD INERTIAL PARAMETERS AND LITERATURE PARAMETERS ($_L$) OF SIX LINKS

Link	L1	L2	L3	L4	L5	L6
M	2.79	19.38	1.94	0.43	3.91	6.01
M_L	2.51	19.08	2.50	0.48	4.03	5.73
Cx	-0.04	-0.03	-0.03	-0.01	-0.05	0.08
Cx_L	0.00	0.00	0.04	0.10	0.00	0.20
Cy	0.01	-0.01	0.02	-0.01	-0.12	-0.02
Cy_L	0.00	0.01	0.10	0.00	0.00	-0.02
Cz	0.01	0.21	-0.03	-0.06	0.40	0.02
Cz_L	0.03	0.23	0.00	0.00	0.16	0.00
Jxx	0.46	0.62	0.02	0.01	0.32	0.04
Jxx_L	0.02	1.38	0.04	0.00	0.12	0.01
Jyy	0.03	0.71	0.03	0.01	0.01	-0.08
Jyy_L	0.01	1.33	0.01	0.01	0.12	0.08
Jzz	-0.01	0.01	0.07	0.01	-0.09	-0.15
Jzz_L	0.02	0.14	0.05	0.01	0.01	0.09

the accuracy of the presumption of prior information, and some constraints on the parameters should be added.

V. CONCLUSION

In this paper we have proposed an identification method for the human body segment parameters. We have shown that is possible to estimate all the standard inertial parameters. The proposed method makes use of 1. the identification of the base parameters and 2. the prior estimated parameters extracted from the data-base of human body. The estimated parameters meet the identification results without distortion, and minimize the error of the prior information from data-base. The proposed approach of RT identification and visualization of results during measurement allows to generate optimal persistent exciting trajectories. However some of the obtained results have shown physically incorrect estimation of the standard parameters. To fix this issue the method requires a more complete data-base for a-priori parameters and to dynamically constrain the center of mass and the principal moment of inertia. Possible applications of the method include interfaces for health monitoring and rehabilitation monitoring, as well as tools for gait analysis and orthopedics.

REFERENCES

[1] C.L. Vaughan, J.C. O'Connor, and B.L. Davis, *Dynamics of human gait*, Human Kinetics Publishers, 1992.

[2] A.L. Betker, T. Szturm, and Z. Moussavi, "Center of mass approximation during walking as a function of trunk and swing leg acceleration," in *Proc. of the 28th IEEE EMBS Annual Int. Conf., New York City, USA*, 2006, pp. 3435–3438.

[3] J. Han, A.L. Betker, T. Szturm, and Z. Moussavi, "Estimation of the center of body mass during forward stepping using body aceleration," in *Proc. of the 28th IEEE EMBS Annual Int. Conf., New York City, USA*, 2006, pp. 4564–4567.

[4] J.W. Young, R.F. Chandler, and C.C. Snow, "Anthropometric and mass distribution characteristics of the adult female," Tech. Rep. FAA-AM-83-16, US Air Force, 1983.

[5] R.K. Jensen, "Estimation of the biomechanical properties of three body types using a photogrammetric method," *J.Biomechanics*, vol. 11, pp. 349–358, 1978.

[6] C.K. Cheng, "Segment inertial properties of chinese adults determined from magnetic resonance imaging," *Clinical biomechanics*, vol. 15, pp. 559–566, 2000.

[7] P. de Leva, "Adjustments to zatsiorsky-seluyanov's segment inertia parameters," *J.of Biomechanics*, vol. 29, no. 9, pp. 1223–1230, 1996.

[8] D.J. Pearsall and P.A. Costigan, "The effect of segment parameter error on gait analysis results," *Gait and Posture*, vol. 9, pp. 173–183, 1999.

[9] G. Venture, K. Ayusawa, and Y. Nakamura, "Motion capture based identification of human inertial parameters," in *Proc. IEEE/EMBS Int. Conf. on Eng. in Medicine and Biology*, 2008, pp. 4575–4578.

[10] G. Venture, K. Ayusawa, and Y. Nakamura, "Dynamics identification of humanoid systems," in *Proc. CISM-IFToMM Symp. on Robot Design, Dynamics, and Control (ROMANSY)*, 2008, pp. 301–308.

[11] K. Ayusawa, G. Venture, and Y. Nakamura, "Inertial parameters identifiability of humanoid robot based on the baselink equation of motion," *Proc. of the Conf. on Robotics and Mechatronics*, 2P1-F09, 2008.

[12] Y. Nakamura, *Advanced Robotics: Redundancy and Optimization*, Addison-Wesley Longman Publishing Co., Inc, 1990.

[13] Y. Yamaguchi, K. Yamane, and Y. Nakamura, "Identification of muscle, tendon, and mass parameters of musculoskeletal human model," *Proc. of the Conf. on Robotics and Mechatronics*, 2A1-D07, 2006.

[14] M. Mochimaru and M. Kouchi, "Japanese body dimension data," *http://riodb.ibase.aist.go.jp/dhbodydb/97-98/index.html.en*, 1997-98.

[15] M. Gautier and W. Khalil, "Exciting trajectories for the identification of base inertial parameters of robots," *Int. J. of Robotic Research*, vol. 11, no. 4, pp. 363–375, 1992.

[16] G. Venture, K. Ayusawa, and Y. Nakamura, "A numerical method for choosing motions with optimal excitation properties for identification of biped dynamics - an application to human," in *Proc. IEEE Int. Conf. on Robotics and Automation (to be published)*, 2009.

[17] G. Venture, P.J. Ripert, W. Khalil, M. Gautier, and P. Bodson, "Modeling and identification of passenger car dynamics using robotics formalism," *IEEE Trans. on Intelligent Transportation Systems*, vol. 7, no. 3, pp. 349–359, 2006.